Inorganic Chemistry

Article

Bridging Nitrate Groups in [Mn$_4$O$_3$(NO$_3$)(O$_2$CMe)$_3$(R$_2$dbm)$_3$] (R = H, Et) and [Mn$_4$O$_2$(NO$_3$)(O$_2$CEt)$_6$(bpy)$_2$](ClO$_4$): Acidolysis Routes to Tetranuclear Manganese Carboxylate Complexes

Guillem Aromí, Sumit Bhaduri, Pau Artús, Kirsten Folting, and George Christou*

Department of Chemistry and Molecular Structure Center, Indiana University, Bloomington, Indiana 47405-7102

New synthesis procedures are described to tetranuclear manganese carboxylate complexes containing the [Mn$_4$O$_2$]$^{8+}$ or [Mn$_4$O$_3$X]$^{6+}$ (X$^-$ = MeCO$_2^-$, F$^-$, Cl$^-$, Br$^-$, NO$_3^-$) core. These involve acidolysis reactions of [Mn$_4$O$_3$(O$_2$CMe)$_4$-(dbm)$_3$] (**1**; dbm is the anion of dibenzoylmethane) or [Mn$_4$O$_2$(O$_2$CEt)$_6$(dbm)$_2$] (**8**) with HX (X$^-$ = F$^-$, Cl$^-$, Br$^-$, NO$_3^-$); high-yield routes to **1** and **8** are also described. The X$^-$ = NO$_3^-$ complexes [Mn$_4$O$_3$(NO$_3$)(O$_2$CR)$_3$(R'$_2$-dbm)$_3$] (R = Me, R' = H (**6**); R = Me, R' = Et (**7**); R = Et, R' = H (**12**)) represent the first synthesis of the [Mn$_4$O$_3$(NO$_3$)]$^{6+}$ core, which contains an unusual η^1:μ_3-NO$_3^-$ group. Treatment of known [Mn$_4$O$_2$(O$_2$CEt)$_7$(bpy)$_2$]-(ClO$_4$) with HNO$_3$ gives [Mn$_4$O$_2$(NO$_3$)(O$_2$CEt)$_6$(bpy)$_2$](ClO$_4$) (**15**) containing a η^1:η^1:μ-NO$_3^-$ group bridging the two body Mn^{III} ions of the [Mn$_4$O$_2$]$^{8+}$ butterfly core. Complex **7**·4CH$_2$Cl$_2$ crystallizes in space group $P2_12_12_1$ with (at −168 °C) a = 21.110(3) Å, b = 22.183(3) Å, c = 15.958(2) Å, Z = 4, and V = 7472.4(3) Å^3. Complex **15**·$^3/_2$CH$_2$Cl$_2$ crystallizes in space group $P2_1/c$ with (at −165 °C) a = 26.025(4) Å, b = 13.488(2) Å, c = 32.102(6) Å, β = 97.27(1)°, Z = 8, and V = 11178(5) Å^3. Complex **7** contains a [Mn$_4$(μ_3-O)$_3$(μ_3-NO$_3$)]$^{6+}$ core (3Mn^{III}, Mn^{IV}) as seen for previous [Mn$_4$O$_3$X]$^{6+}$ complexes. Complex **15** contains a butterfly [Mn$_4$(μ_3-O)$_2$]$^{8+}$ core. ^{1}H NMR spectra have been recorded for all complexes reported in this work and the various resonances assigned. All complexes retain their structural integrity on dissolution in chloroform and dichloromethane. Magnetic susceptibility (χ_M) data were collected on **12** in the 5–300 K range in a 10.0 kG (1 T) field. Fitting of the data to the theoretical χ_M vs T expression appropriate for a [Mn$_4$O$_3$X]$^{6+}$ complex of C_{3v} symmetry gave J_{34} = −23.9 cm^{-1}, J_{33} = 4.9 cm^{-1}, and g = 1.98, where J_{34} and J_{33} refer to the Mn^{III}Mn^{IV} and Mn^{III}Mn^{III} pairwise exchange interactions, respectively. The ground state of the molecule is S = $^9/_2$, as found previously for other [Mn$_4$O$_3$X]$^{6+}$ complexes. This was confirmed by magnetization data collected at various fields and temperatures. Fitting of the data gave S = $^9/_2$, D = −0.45 cm^{-1}, and g = 1.96, where D is the axial zero-field splitting parameter.

Introduction

Manganese carboxylate cluster chemistry is of interest from a variety of viewpoints, including magnetic materials and bioinorganic chemistry. In the former area, it is now well recognized that such clusters often possess large (and sometimes abnormally large) numbers of unpaired electrons, making them attractive as precursors to magnetic materials.[1,2]

Recently, several Mn clusters have been found to demonstrate the new magnetic phenomenon of single-molecule magnetism, the ability of individual molecules to function as magnetizable magnets in the absence of an external magnetic field and with no long-range ordering from intermolecular interactions.[3–5] In the latter area, a tetranuclear Mn cluster is an integral component of the photosystem II (PSII) reaction
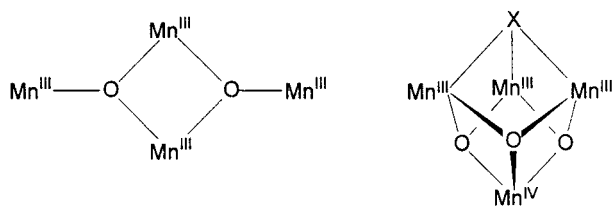
* To whom correspondence should be addressed. Present address: Department of Chemistry, University of Florida, Gainesville, FL 32611-7200. E-mail: christou@chem.ufl.edu.

(1) Christou, G.; Gatteschi, D.; Hendrickson, D. N.; Sessoli, R. *MRS Bull.* **2000**, Nov, 66.

(2) Aromí, G.; Aubin, S. M. J.; Bolcar, M. A.; Christou, G.; Eppley, H. J.; Folting, K.; Hendrickson, D. N.; Huffman, J. C.; Squire, R. C.; Tsai, H.-L.; Wang, S.; Wemple, M. W. *Polyhedron* **1998**, *17*, 3005.

(3) Sessoli, R.; Gatteschi, D.; Caneschi, A.; Novak, M. A. *Nature* **1993**, *365*, 141.

(4) Christou, G. In *Magnetism: A Supramolecular Function*; Kahn, O., Ed.; NATO Series; Kluwer: Dordrecht, The Netherlands, 1996; pp 383–410.

(5) Sessoli, R.; Tsai, H.-L.; Schake, A. R.; Wang, S.; Vincent, J. B.; Folting, K.; Gatteschi, D.; Christou, G.; Hendrickson, D. N. *J. Am. Chem. Soc.* **1993**, *115*, 1804.

center of green plants, where it is responsible for the light-driven oxidation of water to oxygen gas.[6−8] This Mn_4 water oxidation complex (WOC) is the site of substrate (water) binding, deprotonation, and oxidative coupling to O_2, although the precise mechanism is currently unknown. EXAFS data have been of great use to probe the structure of the WOC, and several topological proposals for the arrangement of the Mn ions have been proposed that are consistent with the EXAFS data.[9] During function, the WOC cycles through five oxidation levels labeled S_0–S_4, the highest spontaneously reductively eliminating O_2 and returning to S_0. Recently, crystallographic data have begun to become available on the topological arrangement of the Mn ions of the WOC.[10]

The synthesis and structural and spectroscopic characterization of Mn model complexes have provided a wealth of data for comparison and contrast with those for the native WOC. In our own group over a number of years, we have been devoting a lot of effort to the development of preparative methods to tetranuclear, oxide-bridged manganese carboxylate clusters of potential relevance to the WOC. Among the many complexes synthesized have been complexes with formulas $[Mn_4O_2(O_2CR)_6(py)_2(dbm)_2]$ (dbm is the anion of dibenzoylmethane) and $[Mn_4O_3X(O_2CR)_3(dbm)_3]$,[11−14] displaying the butterfly-like $[Mn_4(\mu_3\text{-}O)_2]^{8+}$ ($4Mn^{III}$) and trigonal pyramidal $[Mn_4(\mu_3\text{-}O)_3(\mu_3\text{-}X)]^{6+}$ ($3Mn^{III}$, Mn^{IV}) cores, respectively, as shown. The latter structure is compat-

ible with one of the topologies based on EXAFS data presented by De Rose et al. for the WOC of PSII.[15] These complexes contain a variable ligand X^-, and to date we have prepared complexes with X^- being Cl^-, Br^-, F^-, N_3^-, OCN^-, $MeCO_2^-$, MeO^-, and OH^-. This site-specific variation has allowed us to assess the influence on the properties of the Mn_4 cluster of small species known to be present at, or to interact with, the native WOC, such as the substrate (H_2O), cofactors (Cl^-, Br^-), inhibitors (F^-), and other molecules similarly relevant to PSII function ($MeOH$, $MeCO_2^-$). One

of the intriguing aspects about the WOC is the influence exerted by the presence of NO_3^-. This anion has a significant effect on the EPR spectrum of the WOC and is capable of substituting for Cl^- as a cofactor and supporting some level of water oxidation activity.[16] As for the native Cl^- cofactor, it is not known whether this ion binds to one or more Mn ions to perform this function. Insights might be provided if appropriate synthetic models were available; however, no higher oxidation state Mn complexes containing nitrate ligands are currently known.

In this paper, we present improved methods to tetranuclear manganese oxo−carboxylate aggregates with the $[Mn_4O_2]^{8+}$ (butterfly) and $[Mn^{III}_3Mn^{IV}O_3(O_2CMe)]^{6+}$ (trigonal pyramidal) cores in high yields and purity. Also, we report new and convenient preparative methods to the $[Mn_4O_3X]^{6+}$ complexes with X = F, Cl, Br, and NO_3 involving acidolysis of either the $[Mn_4O_2]^{8+}$ or $[Mn_4O_3(O_2CMe)]^{6+}$ complex with strong mineral acids HX. The cluster obtained in this way containing a NO_3^- group bound to the core has been prepared for the first time, and it thus allows the initial assessment of ligation tendencies of this ion with high oxidation state Mn centers, and the properties of the resulting product. In addition, acidolysis has provided the first selective substitution of a carboxylate ligand in a butterfly complex with a μ-nitrate group to give $[Mn_4O_2(NO_3)(O_2CEt)_6(bpy)_2](ClO_4)$, and the properties of this complex are also reported.

Experimental Section

Syntheses. Unless otherwise noted, all manipulations were performed under aerobic conditions at ambient temperature using reagents and solvents as received. Stock solutions of 1 M HF, HBr, and HNO_3 in MeCN were prepared by adding the calculated volume of 49% (HF), 48% (HBr), and 69% (HNO_3) aqueous acids containing 0.25 mol of HX to MeCN to a total volume of 250 mL. $NBu^n_4MnO_4$ and $Mn(O_2CEt)_2$ were prepared as described elsewhere.[17,18] dbmH = dibenzoylmethane = 1,3-diphenyl-1,3-propanedione; Et_2dbmH = 4,4′-diethyldibenzoylmethane; bpy = 2,2′-bipyridine.

Et_2dbmH. A dimethoxyethane (150 mL) solution of 4′-ethylacetophenone (7.9 mL, 51 mmol) and ethyl 4-ethylbenzoate (9.17 g, 51 mmol) was introduced under argon into a flask containing pure NaH (2.59 g, 108 mmol). The yellow mixture was brought to reflux, resulting in the evolution of gas as the system turned darker and thicker. After 2 h, the system was allowed to cool to room temperature, and stirring was maintained overnight. Upon addition of water (∼100 mL), the thick mixture turned into a dark brown solution, and this was treated with ∼10% HCl until acidic pH was reached. Et_2O (∼200 mL) was added to obtain two separate phases. The organic phase was worked up as usual to give a yellow oil after rotary evaporation, and this was dissolved in EtOH (60 mL) and treated with $Cu(AcO)_2\cdot H_2O$ (5.6 g, 112 mmol). The green mixture was stirred at 60−70 °C for 3 h and then at room temperature overnight, after which a green precipitate was collected by filtration, and washed with copious EtOH and Et_2O. A slurry of this precipitate in Et_2O (15 mL) was treated with 36% HCl until

(6) Yachandra, V. K.; Sauer, K.; Klein, M. P. *Chem. Rev.* **1996**, *96*, 2927.
(7) *Manganese Redox Enzymes*, Pecoraro, V. L., Ed.; VCH Publishers: New York, 1992.
(8) Penner-Hahn, J. E. *Struct. Bonding* **1998**, *90*, 1.
(9) Yachandra, V. K.; DeRose, V. J.; Latimer, M. J.; Mukherji, I.; Sauer, K.; Klein, M. P. *Science* **1993**, *260*, 675.
(10) Zouni, A.; Witt, H.-T.; Kern, J.; Fromme, P.; Krauss, N.; Saenger, W.; Orth, P. *Nature* **2001**, *409*, 739.
(11) Wemple, M. W.; Adams, D. M.; Hagen, K. S.; Folting, K.; Hendrickson, D. N.; Christou, G. *J. Chem. Soc., Chem. Commun.* **1995**, 1591.
(12) Wemple, M. W.; Tsai, H.-L.; Folting, K.; Hendrickson, D. N.; Christou, G. *J. Am. Chem. Soc.* **1995**, *117*, 7275.
(13) Wemple, M. W.; Adams, D. M.; Folting, K.; Hagen, K. S.; Hendrickson, D. N.; Christou, G. *Inorg. Chem.*, to be submitted for publication.
(14) Aromí, G.; Wemple, W. M.; Aubin, J. S.; Folting, K.; Hendrickson, N. D.; Christou, G. *J. Am. Chem. Soc.* **1998**, *120*, 5850.
(15) Derose, V. J.; Mukerji, I.; Latimer, M. J.; Yachandra, V. K.; Sauer, K.; Klein, M. P. *J. Am. Chem. Soc.* **1994**, *116*, 5239.
(16) Ono, T.; Nakayama, H.; Gleiter, H.; Inoue, Y.; Kawamori, A. *Arch. Biochem. Biophys.* **1987**, *256*, 618.
(17) Vincent, J. B.; Folting, K.; Huffman, J. C.; Christou, G. *J. Am. Chem. Soc.* **1986**, *25*, 996.
(18) Aromí, G.; Bhaduri, S.; Artús, P.; Yoo, J.; Huffman, J. C.; Hendrickson, D. N.; Christou, G., submitted for publication to *Polyhedron*.

the solid dissolved and two phases separated. The organic phase was rotary evaporated to obtain a yellow oil which turned into solid Et_2dbmH when put under vacuum. The yield was 60%. ^1H NMR ($CDCl_3$): triplet (6H), 1.29 ppm; quadruplet (4H), 2.74 ppm; singlet (1H), 6.83 ppm; doublet (4H), 7.33 ppm; doublet (4H), 7.93 ppm; singlet (1H), 16.99 ppm. Anal. Calcd (Found) for $Et_2dbmH\cdot$ $0.25H_2O$: C, 80.11 (80.37); H, 7.25 (7.72). CIMS: m/z 280 (M$^+$, 5), 135 (70), 119 (24), 105 (100), 91 (64), 77 (66).

[$Mn_4O_3(O_2CMe)_4(dbm)_3$] (1). A solution of $Mn(O_2CMe)_2\cdot4H_2O$ (4.00 g, 16.3 mmol) in water (46 mL) was added to a solution of dbmH (3.47 g, 15.5 mmol) in glacial acetic acid (316 mL). To the resulting yellow solution was added dropwise a purple solution of $KMnO_4$ (942 mg, 5.96 mmol) in water (78 mL) to yield a dark brown solution from which a brown solid started to precipitate. The mixture was stirred for about 3 h and filtered. The powder obtained was washed with MeCN and Et_2O, and dried in air. Yields of 50−70% based on total Mn were obtained. Complex **1** was recrystallized by layering a CH_2Cl_2 solution with MeCN. Anal. Calcd (Found) for **1**$\cdot0.4CH_2Cl_2$: C, 53.11 (53.35); H, 3.82 (3.50); N, 0.00 (0.07).

[$Mn_4O_3(O_2CMe)_4(Et_2dbm)_3$] (2). To a brown slurry of [$Mn_3O(O_2$-$CMe)_6$]($MeCO_2$) (500 mg, 0.86 mmol) in MeCN (15 mL) and glacial acetic acid (2 mL) were simultaneously added dropwise two separate solutions of Et_2dbmH (613 mg, 2.19 mmol) in MeCN (10 mL) and NBu_4MnO_4 (73 mg, 0.20 mmol) in MeCN (1 mL). The mixture was stirred for 15 min, and then a brown powder was collected by filtration. This was stirred in CH_2Cl_2 (10 mL) for 10 min, undissolved solid removed by filtration, and the filtrate concentrated to a solid by rotoevaporation. The brown residue was slurried with Et_2O, collected by filtration, washed with Et_2O, and dried in air. The yield was 45% based on total Mn. Anal. Calcd (Found) for **2**$\cdot0.2MeCN\cdot1.6Et_2O$: C, 57.33 (57.63); H, 5.74 (5.44); N, 0.19 (0.22).

[$Mn_4O_3Cl(O_2CMe)_3(dbm)_3$] (3). To a solution of complex **1** (0.20 g, 0.17 mmol) in CH_2Cl_2 (40 mL) was added 37% aqueous HCl (41 μL, ∼0.5 mmol) diluted in MeCN (∼2 mL). The solution was stirred for about 25 min, whereupon a fine orange-brown solid started to precipitate. Et_2O (30 mL) was added to complete precipitation, and the solid was collected by filtration, washed with Et_2O, and dried in air. The yield of complex **3** was 76%.

[$Mn_4O_3Br(O_2CMe)_3(dbm)_3$] (4). To a solution of complex **1** (0.20 g, 0.17 mmol) in CH_2Cl_2 (40 mL) was added 680 μL of a 1 M MeCN solution of HBr (0.68 mmol). The solution was decanted into a clean flask to remove the water droplets that separated out of the bottom, and after a further 30 min, a fine orange-brown product was precipitated by addition of Et_2O (50 mL). The solid was collected by filtration, washed with Et_2O, and dried in air. The yield of complex **4** was 51%.

[$Mn_4O_3F(O_2CMe)_3(dbm)_3$] (5). To a slurry of complex **1** (0.20 g, 0.17 mmol) in CH_2Cl_2 (20 mL) was added 340 μL of a 1 M MeCN solution of HF (0.34 mmol). The slurry converted to a dark brown solution as the solid dissolved, and this was stirred for a further 30 min. An orange microcrystalline solid was then precipitated by addition of hexanes (50 mL), and this was collected by filtration, washed with Et_2O, and dried in air. The yield of complex **5** was 84%.

[$Mn_4O_3(NO_3)(O_2CMe)_3(dbm)_3$] (6). Method 1. To a stirred solution of complex **1** (0.2 g, 0.17 mmol) in CH_2Cl_2 (30 mL) was added 340 μL of a 1 M MeCN solution of HNO_3 (0.34 mmol). After 25 min, an orange-brown solid was precipitated from solution by addition of Et_2O (50 mL), and this was collected by filtration, washed with Et_2O, and dried in air. The yield of complex **6** was 66%.

Method 2. To a slurry of complex **1** (0.10 g, 0.085 mmol) in CH_2Cl_2 (18 mL) was added a solution of NEt_4NO_3 (0.38 mmol) and F_3CSO_2OH (0.20 mmol) in MeCN (1.45 mL). The mixture was stirred for about 8 min and concentrated in vacuo. Et_2O was used to form a slurry, and the solid was collected by filtration, washed with copious MeCN and Et_2O, and dried in vacuo. The yield was 61%. Anal. Calcd (Found) for **6**$\cdot0.5MeCN$: C, 52.2 (51.9); H, 4.1 (3.9); N, 1.7 (1.7).

[$Mn_4O_3(NO_3)(O_2CMe)_3(Et_2dbm)_3$] (7). Method 1. To a solution of complex **2** (150 mg, 0.112 mmol) in CH_2Cl_2 (10 mL) was added 226 μL of a 1 M MeCN solution of HNO_3 (0.34 mmol), and the mixture was stirred for about 10 min. Addition of Et_2O (70 mL) and hexanes (30 mL) led to the precipitation of a brown powder which was collected by filtration, washed with Et_2O, and dried in vacuo. The yield was 45%. Anal. Calcd (Found) for **7**$\cdot0.7CH_2Cl_2$: C, 55.63 (55.36); H, 5.16 (5.15); N, 1.02 (1.12).

Method 2. To a solution of complex **2** (72 mg, 0.054 mmol) in CH_2Cl_2 (10 mL) was added a solution of NEt_4NO_3 (0.27 mmol) and F_3CSO_2OH (0.14 mmol) in MeCN (1 mL). The mixture was stirred for about 10 min and concentrated in vacuo. Et_2O was used to form a slurry, and the solid was collected by filtration, washed with copious MeCN and Et_2O, and dried in vacuo. The yield was 30%. Crystals of complex **1** suitable for X-ray crystallography were obtained by layering a CH_2Cl_2 (2 mL) solution of the compound (20 mg) with hexanes over 5 days at room temperature.

[$Mn_4O_2(O_2CEt)_6(dbm)_2$] (8). A solution of $Mn(O_2CEt)_2\cdot4H_2O$ (568 mg, 2.08 mmol) in H_2O (6 mL) was added to a solution of dbmH (460 mg, 2.08 mmol) in propionic acid (30 mL). To the resulting yellow solution was added dropwise a purple solution of $KMnO_4$ (120 mg, 0.76 mmol) in H_2O (10 mL) to yield a dark brown solution from which a light brown solid started to precipitate immediately. When precipitation was judged to be complete, the product was collected by filtration, washed with Et_2O, and dried in vacuo. Complex **8** was recrystallized by stirring 200 mg of the crude product with 20 mL of MeCN for ∼20 min. The resulting dark brown microcrystalline solid was collected by filtration, washed with Et_2O, and dried in vacuo. The overall yield was 86% based on total Mn. Anal. Calcd (Found) for **8**: C, 50.72 (50.69); H, 4.61 (4.73). Crystals of **8**$\cdot$hexane suitable for X-ray crystallography were obtained by layering a solution of the compound (400 mg) in CH_2Cl_2 (20 mL) with hexanes.

[$Mn_4O_3Cl(O_2CEt)_3(dbm)_3$] (9). To a solution of **8** (0.20 g, 0.18 mmol) in CH_2Cl_2 (7 mL) was added 37% aqueous HCl (28 μL, ∼0.34 mmol) diluted in MeCN (∼2 mL). The solution was stirred for about 3 min, and then Et_2O (30 mL) was added. The mixture was left undisturbed for ∼6 h, during which time small black crystals formed. These were collected by filtration, washed with MeCN and Et_2O, and dried in vacuo. The yield was 66% based on the limiting reagent (dbm$^-$). Anal. Calcd (Found) for **9**$\cdot0.8CH_2Cl_2$: C, 52.23 (52.10); H, 3.97 (4.00); N, 0.00 (0.00).

[$Mn_4O_3Br(O_2CEt)_3(dbm)_3$] (10). To a solution of complex **8** (0.40 g, 0.35 mmol) in CH_2Cl_2 (14 mL) was added 1.02 mL of a 1 M MeCN solution of HBr (1.02 mmol). The solution was decanted into a different flask to remove the water droplets that deposited at the bottom. The solution was stirred for ∼3 min, Et_2O (60 mL) added, and the flask left undisturbed overnight at room temperature. The resulting black crystals were collected by filtration, washed with MeCN and Et_2O, and dried in vacuo. The yield was 35% based on dbm$^-$. Anal. Calcd (Found) for **10**$\cdot0.4CH_2Cl_2$: C, 51.42 (51.40), H, 3.87 (3.71); N, 0.00 (0.00).

[$Mn_4O_3F(O_2CEt)_3(dbm)_3$] (11). To a solution of complex **8** (0.40 g, 0.35 mmol) in CH_2Cl_2 (20 mL) was added 1.06 mL of a 1 M MeCN solution of HF (1.06 mmol). The solution was stirred

for ~3 min, Et_2O (110 mL) added, and the flask left undistured at room temperature overnight. The resulting small, dark brown crystals were collected by filtration, washed with MeCN and Et_2O, and dried in air. This solid was stirred in CH_2Cl_2 (16 mL) for about 30 min, a small amount of insoluble brown powder was removed by filtration, and Et_2O (40 mL) was added to the filtrate. The flask was left overnight at room temperature, and the resulting small crystals were collected by filtration, washed with Et_2O, and dried in vacuo. The yield was 38% based on dbm⁻. Anal. Calcd (Found) for **11**·0.2CH₂Cl₂: C, 54.58 (54.38); H, 4.09 (4.39); N, 0.00 (0.00).

[Mn₄O₃(NO₃)(O₂CEt)₃(dbm)₃] (12). To a slurry of complex **8** (0.40 g, 0.35 mmol) in MeCN (25 mL) was added 1.08 mL of a 1 M MeCN solution of HNO_3 (1.08 mmol). The slurry turned into a dark brown solution from which orange-brown microcrystals precipitated almost immediately. The mixture was stirred for about 25 min, and the solid was collected by filtration, washed with MeCN and Et_2O, and dried in vacuo. The yield was 31% based on dbm⁻. Anal. Calcd (Found) for **12**: C, 53.22 (53.06); H, 3.97 (3.88); N, 1.15 (1.02).

(NBu₄)[Mn₄O₂(O₂CEt)₇(pic)₂] (13). A solution of $Mn(O_2CEt)_2$·4H₂O (757 mg, 2.77 mmol) in H_2O (5 mL) was added to a solution of picH (256 mg, 2.08 mmol) and NBu₄ClO₄ (260 mg, 0.76 mmol) in propionic acid (30 mL). To the resulting yellow solution was added dropwise a purple solution of NBu₄MnO₄ (274 mg, 0.76 mmol) in MeCN (2 mL) to yield a red-brown solution which was stirred for ~3 h. Addition of Et_2O (200 mL) led to the formation of a red precipitate which was collected by filtration, washed with Et_2O, and dried in air. The yield was 85% based on total Mn. Anal. Calcd (Found) for **13**·0.5H₂O: C, 46.75 (46.39); H, 6.41 (6.09); N, 3.34 (3.69).

[Mn₄O₂(O₂CEt)₇(bpy)₂](ClO₄) (14). A solution of $Mn(O_2CEt)_2$·4H₂O (757 mg, 2.77 mmol) in water (6 mL) was mixed with a solution of bpy (325 mg, 2.08 mmol) and NBu₄ClO₄ (520 mg, 1.52 mmol) in propionic acid (25 mL). To the resulting yellow solution was added dropwise a purple solution of NBu₄MnO₄ (274 mg, 0.76 mmol) in MeCN (2 mL) to yield a red solution which was stirred for about 2 h. Addition of Et_2O (200 mL) led to precipitation of a microcrystalline red product which was collected by filtration, washed with Et_2O, and dried in vacuo. The yield was 81% based on total available Mn. Anal. Calcd (Found) for **14**·0.4EtCO₂H: C, 42.07 (41.97); H, 4.47 (4.34); N, 4.65 (4.37).

[Mn₄O₂(NO₃)(O₂CEt)₆(bpy)₂](ClO₄) (15). To a red solution of **14** (300 mg, 0.255 mmol) in MeCN (15 mL) was added a MeCN solution of HNO_3 (255 μL, 1 M, 0.255 mmol). The solution was left undisturbed for 2−3 h, during which time dark orange needles were slowly deposited. The product was collected by filtration, washed with Et_2O, and dried in vacuo. The yield was 64%. Anal. Calcd (Found) for **15**: C, 39.21 (39.02); H, 3.98 (4.12); N, 6.02 (6.04).

X-ray Crystallography and Structure Solution. Data were collected on a Picker four-circle diffractometer at ~−170 °C; details of the diffractometry, low-temperature facilities, and computational procedures employed by the Molecular Structure Center are available elsewhere.[19] Small black crystals suitable for X-ray diffraction were selected from the bulk samples (maintained in mother liquor to prevent rapid solvent loss) and transferred to the goniostat, where they were cooled for characterization and data collection ($6° \leq 22° \leq 45°$, +h, +k, +l for **7**·xCH₂Cl₂; and $6° \leq 22° \leq 50°$, +h, +k, ±l for **15**·³/₂CH₂Cl₂). Systematic searches of limited hemispheres of reciprocal space and analysis using the

programs DIRAX and TRACER revealed an orthorhombic unit cell for **7**·xCH₂Cl₂ and a monoclinic unit cell for **15**·³/₂CH₂Cl₂. Following data collection, the systematic absences uniquely identified the space groups as $P2_12_12_1$ for **7**·xCH₂Cl₂ and $P2_1/c$ for **15**·³/₂CH₂Cl₂. The structures were solved by direct methods (MULTAN78) and Fourier techniques, and refined on F by full-matrix least-squares.

For **7**·xCH₂Cl₂, the positions of the four Mn atoms were obtained in the initial E-map and the remaining non-hydrogen atoms were located in iterations of least-squares refinement, followed by a difference Fourier map calculation. Hydrogen atoms were introduced in fixed, calculated positions with isotropic thermal parameters equal to 1.0 plus the isotropic equivalent of the parent atom. Disorder was observed in two of the ethyl groups, C41 and C41′, which refined to 45% and 55% occupancy, respectively, while C62 and C62′ refined to 70% and 30%, respectively. Hydrogen atoms were not calculated for C40, C41, C41′, C61, C62, and C62′. The asymmetric unit also contained very disordered solvent molecules, assumed to be CH_2Cl_2, which had been used in the crystallization. A total of 18 atoms (16 Cl atoms and 2 C atoms) of varying occupancy were found for the solvent molecules. The final full-matrix least-squares refinement was carried out using anisotropic thermal parameters on atoms in the main molecule, except for the disordered atoms, which were kept isotropic. The final difference Fourier contained several peaks of about 1 e/Å³ in the areas of the disordered solvent molecules. The deepest hole was −0.63 e/Å³.

For **15**·³/₂CH₂Cl₂, an analytical absorption correction was carried out and the structure was solved using DIRDIF-96, a program combining Patterson and direct methods. All non-hydrogen atoms were readily located. The asymmetric unit contains two almost identical Mn₄ cations, two ClO₄⁻ anions, three molecules of CH_2Cl_2, and seven atoms from an unidentified solvent, possibly hexane; the occupancies of the latter varied from 45% to 93%. A small (50/50) disorder in one of the propionate groups (C15/C15A) was observed. Hydrogen atoms were introduced as for **7**·xCH₂Cl₂, except for on the disordered atoms. During the initial anisotropic refinement, atoms C22, C29, C78, C110, C115, and C126 did not converge properly to the anisotropic form and were kept isotropic. The disordered atoms and the unidentified solvent atoms were also refined isotropically. The final refinement was carried out using anisotropic thermal parameters on all non-hydrogen atoms (except as above). The final difference Fourier map was essentially featureless, the largest peak being 1.17 e/Å³ from a hexane atom. The deepest hole was −1.08 e/Å³.

Final R (R_w) indices for the two complexes are included in Table 1.

Physical Measurements. Infrared spectra were recorded as KBr disks or Nujol mulls between KBr plates on a Nicolet Model 510P spectrophotometer. ¹H NMR spectroscopy was performed on a 300 MHz Varian Gemini 2000 NMR spectrometer with the protio solvent signal used as reference, and ²H NMR spectra were collected on a 400 MHz Varian Inova NMR spectrometer with the deuterio solvent signal used as reference. dc magnetic susceptibility data were collected on powdered, microcrystalline samples on a Quantum Design MPMS-XL SQUID magnetometer equipped with a 7 T (70 kG) magnet. A diamagnetic correction to the observed susceptibilities was applied using Pascal's constants. Elemental analyses were performed by Atlantic Microlab or at Indiana University using a Perkin-Elmer Series II CHNS/O Analyzer 2000.

Results

Preparation of Tetranuclear Complexes via Comproportionation. Comproportionation reactions between Mn^{II}
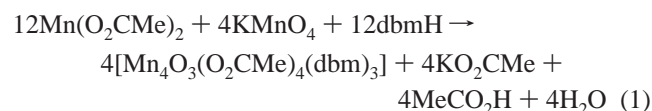
(19) Chisholm, M. H.; Folting, K.; Huffman, J. C.; Kirkpatrick, C. C. *Inorg. Chem.* **1984**, *23*, 1021.

Table 1. Crystallographic Data for **7** and **15**

	7	**15**
empirical formula	$C_{67}H_{74}Cl_8Mn_4NO_{18}$[a]	$C_{39.5}H_{49}Cl_4Mn_4N_5O_{21}$[b]
fw	1684.69	1291.41
space group	$P2_12_12_1$	$P2_1/c$
a, Å	21.110(3)	26.025(4)
b, Å	22.183(3)	13.488(2)
c, Å	15.958(2)	32.102(6)
β, deg	90	97.27(1)
V, Å^3	7472.4(3)	11178(5)
Z	4	8
T, °C	−168	−165
radiation,[c] Å	0.71069	0.71069
ρ_{calcd}, g/cm^3	1.498	1.535
μ, cm^{-1}	10.125	11.487
R (R_w),[d,e] %	7.48 (7.35)	8.6 (7.6)

[a] Including four CH$_2$Cl$_2$ solvate molecules. [b] Including 1.5 CH$_2$Cl$_2$ solvate molecules. [c] Graphite monochromator. [d] $R = 100\sum||F_o| - |F_c||/\sum|F_o|$. [e] $R_w = 100[\sum w(|F_o| - |F_c|)^2/\sum w|F_o|^2]^{1/2}$, where $w = 1/\sigma^2(|F_o|)$.
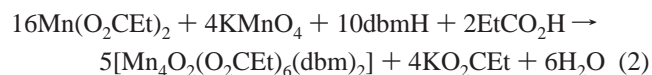
and Mn^{VII} sources have found extensive use in our group to produce Mn/O/RCO$_2$ aggregates of various nuclearities. For example, [Mn$_3$O(O$_2$CR)$_6$(py)$_3$]$^{0,+}$ complexes are readily obtained from Mn^{II} and MnO$_4$$^-$ in organic solvents.[20] In some cases, these clusters are useful starting points from which to access species of higher nuclearity. Thus, addition of the appropriate chelate ligand to [Mn$_3$O(O$_2$CMe)$_6$(py)$_3$](ClO$_4$)[17] leads to [Mn$_4$O$_2$(O$_2$CMe)$_7$(pic)$_2$]$^-$,[21] [Mn$_4$O$_2$(O$_2$CMe)$_7$(bpy)$_2$]$^+$,[22] and [Mn$_4$O$_2$(O$_2$CMe)$_6$(py)$_2$(dbm)$_2$][23] (picH = picolinic acid; bpy = 2,2′-bipyridine; dbmH = dibenzoylmethane). In a combination of these two approaches, (NBu$^n_4$)[Mn$_4$O$_2$(O$_2$CMe)$_7$(pic)$_2$] and [Mn$_4$O$_2$(O$_2$CPh)$_7$(bpy)$_2$](ClO$_4$) were obtained directly via comproportionation in the presence of pic$^-$ and bpy, respectively, as well as the corresponding carboxylate.[21] The present results arise from an attempted extension of this direct approach to reactions involving dbmH, but these were surprisingly found to yield higher oxidation state complexes. Thus, addition of aqueous KMnO$_4$ to a solution of Mn(O$_2$CMe)$_2$·2H$_2$O and dbmH in glacial acetic acid led to [Mn$_4$O$_3$(O$_2$CMe)$_4$(dbm)$_3$] (**1**), a Mn$^{III}_3$Mn^{IV} product. The formation of **1** is summarized in eq 1. This represents a vastly superior route to complex **1**,

$$12Mn(O_2CMe)_2 + 4KMnO_4 + 12dbmH \rightarrow$$
$$4[Mn_4O_3(O_2CMe)_4(dbm)_3] + 4KO_2CMe +$$
$$4MeCO_2H + 4H_2O \quad (1)$$

which had been previously prepared only on a small scale by controlled potential electrolysis of [Mn$_4$O$_2$(O$_2$CMe)$_6$(py)$_2$(dbm)$_2$] under anaerobic conditions.[12,23] This compound has served in the past as an excellent starting point for preparing the derivatives [Mn$_4$O$_3$X(O$_2$CMe)$_3$(dbm)$_3$] (X = F,[12] Cl,[13] Br,[13] OMe,[14] OH,[14] N$_3$[13]), which constitute an isostructural series of single-molecule magnets.[24] The facile, high-scale synthesis of complex **1** reported here has also enabled the

study of this family of compounds using techniques such as inelastic neutron scattering (INS), which requires several grams of material.[25]

If the same reaction is carried out in propionic acid using Mn(O$_2$CEt)$_2$ instead of Mn(O$_2$CMe)$_2$, the new complex [Mn$_4$O$_2$(O$_2$CEt)$_6$(dbm)$_2$] (**8**) precipitates from the reaction mixture (eq 2). Complex **8** is a 4Mn^{III} product and is structurally different from **1**. The fact that the complex analogous to **1** is not formed is ascribed to the low solubility of **8**.

$$16Mn(O_2CEt)_2 + 4KMnO_4 + 10dbmH + 2EtCO_2H \rightarrow$$
$$5[Mn_4O_2(O_2CEt)_6(dbm)_2] + 4KO_2CEt + 6H_2O \quad (2)$$

Similar reactions were also carried out with picolinic acid and bipyridine. Thus, addition of a MeCN solution of NBu$^n_4$-MnO$_4$ to Mn(O$_2$CEt)$_2$ and picH in propionic acid gave the 4Mn^{III} complex (NBu$^n_4$)[Mn$_4$O$_2$(O$_2$CEt)$_7$(pic)$_2$] (**13**). The preparation of **13** is very similar to that previously reported for the MeCO$_2$$^-$ derivative, but the yield is significantly higher (85% vs 46%), and no further purification steps are needed. With bpy in the presence of NBu$^n_4$ClO$_4$, the expected compound, [Mn$_4$O$_2$(O$_2$CEt)$_7$(bpy)$_2$](ClO$_4$) (**14**), was obtained in 80% yield and high purity. Complex **14** is analogous to previously reported [Mn$_4$O$_2$(O$_2$CMe)$_7$(bpy)$_2$](ClO$_4$).[22]

Acidolysis Reactions of 1 and 8. Complex **1** contains three η^2:μ_2-MeCO$_2$$^-$ groups and one η^1:μ_3-MeCO$_2$$^-$ group bridging the three Mn^{III} ions. The latter carboxylate can be selectively replaced by other ligands in site-specific ligand substitution reactions to produce a family of compounds [Mn$_4$O$_3$X(O$_2$CMe)$_3$(dbm)$_3$] (X = F, Cl, Br, N$_3$).[11−13] These were formed by electrophilic attack on the η^1:μ_3-AcO$^-$ group by reagents capable of delivering the incoming ligand, i.e., Me$_3$SiX (X = Cl, Br, N$_3$) and Et$_2$NSF$_3$ (X = F).

We have been interested for some time in studying the interaction of NO$_3$$^-$ with tetranuclear manganese clusters, since this anion has been found to alter the EPR signal of the WOC in PSII, and to partially restore the activity of the enzyme in Cl$^-$-depleted samples.[16] We believed that replacement of the η^1:μ_3-MeCO$_2$$^-$ group of complex **1** by NO$_3$$^-$ might be a suitable route to a Mn$_4$/NO$_3$ species. Since a nitrate-containing reagent of the kind described above was not available, we explored the protonation of the η^1:μ_3-MeCO$_2$$^-$ group of **1** in the presence of nitrate, using a strong acid of a noncoordinating anion in combination with an organic source of nitrate. The reaction of complex **1** with CF$_3$SO$_2$OH and NEt$_4$NO$_3$ was monitored by ^{2}H NMR spectroscopy using [Mn$_4$O$_3$(CD$_3$CO$_2$)$_4$(dbm)$_3$] (**1a**). The ^{2}H NMR spectrum of **1a** shows, in addition to the signal from the solvent, two peaks at 36.8 and 66.1 ppm corresponding to the three equivalent η^2:μ_2-(CD$_3$CO$_2$$^-$) groups and the unique η^1:μ_3-(CD$_3$CO$_2$$^-$) group, respectively (Figure 1, top). Addition of a slight excess of CF$_3$SO$_2$OH and NEt$_4$NO$_3$ in MeCN causes a slight shift of the first signal and the

(20) Lis, T. *Acta Crystallogr., Sect. B* **1980**, *36*, 2042.

(21) Libby, E.; McCusker, J. K.; Schmitt, E. A.; Folting, K.; Hendrickson, D. N.; Christou, G. *Inorg. Chem.* **1991**, *30*, 3486.

(22) Vincent, J. B.; Christmas, C.; Chang, H.-R.; Li, Q.; Boyd, P. D. W.; Huffman, J. C.; Hendrickson, D. N.; Christou, G. *J. Am. Chem. Soc.* **1989**, *111*, 2086.

(23) Wang, S. Wemple, M. W., Yoo, J.; Folting, K.; Huffman, J. C.; Hagen, K. S.; Hendrickson, D. N.; Christou, G. *Inorg. Chem.* **2000**, *39*, 1501.

(24) Aubin, S.; Wemple, M. W.; Adams, D. M.; Tsai, H.-L.; Christou, G.; Hendrickson, D. N. *J. Am. Chem. Soc.* **1996**, *118*, 7746.

(25) Andres, H.; Basler, R.; Güdel, H.-U.; Aromí, G.; Christou, G.; Büttner, H.; Rufflé, B. *J. Am. Chem. Soc.* **2000**, *122*, 12469.
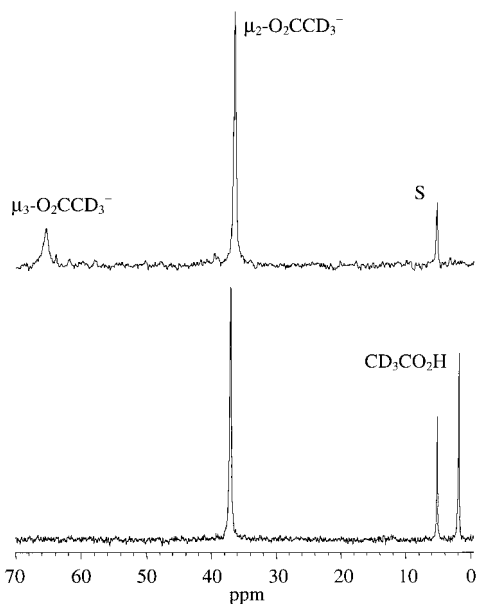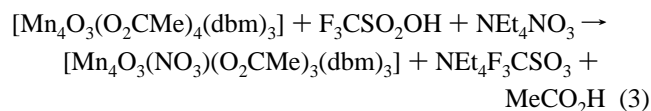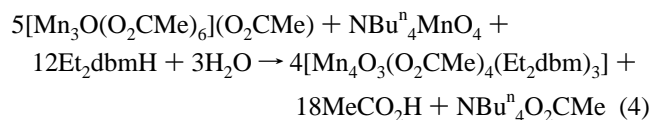
Figure 1. ^{2}H NMR (400 MHz) spectra in CH_2Cl_2 of **1a** (top) and **6a** (bottom) generated in situ in the NMR tube (see the text for details). The small amount of naturally occurring $CDHCl_2$ (S) is used as an internal reference.

disappearance of the second one. In addition, a peak at ~2 ppm corresponding to free CD_3CO_2H appears (Figure 1, bottom). These observations are consistent with the replacement of the unique acetate group by nitrate to form the product $[Mn_4O_3(NO_3)(O_2CCD_3)_3(dbm)_3]$ (**6a**). The reaction (eq 3) was therefore performed on a large scale, and the nitrate-substituted complex $[Mn_4O_3(NO_3)(O_2CMe)_3(dbm)_3]$ (**6**) was successfully isolated and characterized.

$$[Mn_4O_3(O_2CMe)_4(dbm)_3] + F_3CSO_2OH + NEt_4NO_3 \rightarrow$$
$$[Mn_4O_3(NO_3)(O_2CMe)_3(dbm)_3] + NEt_4F_3CSO_3 +$$
$$MeCO_2H \quad (3)$$

X-ray structural confirmation of the binding of NO_3^- (vide infra) was obtained using the related complex $[Mn_4O_3(NO_3)\text{-}(O_2CMe)_3(Et_2dbm)_3]$ (**7**), which contains a *p*-ethyl-substituted version of the dbm$^-$ ligand. The crystal structure revealed the presence of a $\eta^1:\mu_3\text{-}NO_3^-$ ligand bridging three Mn^{III} centers, providing the first example of this coordination mode for NO_3^-. Complex **7** was prepared analogously to **6**, using $[Mn_4O_3(O_2CMe)_4(Et_2dbm)_3]$ (**2**). Complex **2** had itself never been made before, and it was obtained by oxidation in MeCN of the polymeric complex $[Mn_3O(O_2CMe)_6](MeCO_2)$ with $NBu^n_4MnO_4$ in the presence of Et$_2$dbmH and $MeCO_2H$, as summarized in eq 4.

$$5[Mn_3O(O_2CMe)_6](O_2CMe) + NBu^n_4MnO_4 +$$
$$12Et_2dbmH + 3H_2O \rightarrow 4[Mn_4O_3(O_2CMe)_4(Et_2dbm)_3] +$$
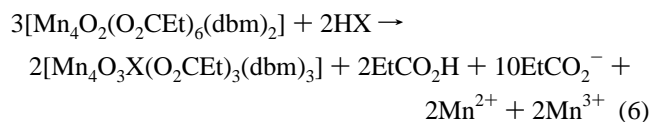$$18MeCO_2H + NBu^n_4O_2CMe \quad (4)$$

The successful use of triflic acid and NEt_4NO_3 to effect site-specific ligand substitution in complexes **1** and **2** suggested that the use of just strong aqueous mineral acids in the appropriate stoichiometry might lead to similar results.

Thus, 1 M MeCN solutions of the concentrated acids aqueous HCl (37%), aqueous HBr (48%), aqueous HF (49%), and aqueous HNO$_3$ (69%) were prepared. When amounts of HX (X = Cl, Br, F, NO$_3$) ranging from 2 to 4 equiv (see the Experimental Section) were added to CH_2Cl_2 solutions of **1**, the corresponding $[Mn_4O_3X(O_2CMe)_3(dbm)_3]$ complexes (X = Cl, **3**; Br, **4**; F, **5**; NO$_3$, **6**) were formed and isolated in good yields, according to eq 5. In all cases, an excess of

$$[Mn_4O_3(O_2CMe)_4(dbm)_3] + HX \rightarrow$$
$$[Mn_4O_3X(O_2CMe)_3(dbm)_3] + MeCO_2H \quad (5)$$
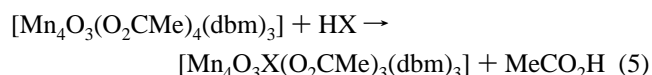
acid (2−4 equiv) was needed to drive the reaction to completion, without causing major decomposition. In addition to providing a second route to the nitrate-bridged complex **6**, this method has also afforded a new and convenient way to prepare known complexes **3**−**5** on a large scale.

Acidolysis reactions with **8** were also investigated. We have shown in earlier reports[11,26,27] that removal of bridging carboxylate ligands from the complex $[Mn_4O_2(O_2CMe)_6(py)_2\text{-}(dbm)_2]$ with Me_3SiX (X = Cl, Br, N$_3$, N-bound OCN) leads to a core rearrangement and disproportionation to give the corresponding μ_3-X-containing molecules $[Mn_4O_3X\text{-}(O_2CMe)_3(dbm)_3]$ (3Mn^{III}, Mn^{IV}). To explore whether such reactions could also be triggered by mineral acids HX, where carboxylate removal would take place by protonation, or whether the cluster would be destroyed by the acid conditions, CH_2Cl_2 solutions of complex **8** were treated with 2−3 equiv (see the Experimental Section) of HX (X = Cl, Br, F, NO$_3$), followed by the addition of Et$_2$O. The complexes $[Mn_4O_3X(O_2CEt)_3(dbm)_3]$ (Cl, **9**; Br, **10**; F, **11**) crystallized overnight from the reaction mixtures. The reaction with HNO$_3$ yielded the analogous NO$_3^-$-containing compound along with a coproduct (as revealed by ^{1}H NMR and IR spectroscopy). Attempts to separate the two species were unsuccessful. However, if the HNO$_3$ solution was added to a MeCN slurry of complex **8**, a reaction took place within minutes and pure $[Mn_4O_3(NO_3)(O_2CEt)_3(dbm)_3]$ (**12**) precipitated. These reactions presumably involve a process of core disproportionation and rearrangement analogous to that in the Me_3SiX reactions[11,26,27] (vide supra). The transformation is summarized in eq 6.

$$3[Mn_4O_2(O_2CEt)_6(dbm)_2] + 2HX \rightarrow$$
$$2[Mn_4O_3X(O_2CEt)_3(dbm)_3] + 2EtCO_2H + 10EtCO_2^- +$$
$$2Mn^{2+} + 2Mn^{3+} \quad (6)$$

The above results demonstrate the instability of the $[Mn_4O_2]^{8+}$ core of **8** toward the removal of one or more bridging carboxylate ligands. To effect the selective substitution of a single bridging carboxylate group by NO$_3^-$ from a $[Mn_4O_2]^{8+}$ complex *without* modifying the core, compound **14** seemed a better starting material. This molecule has a

(26) Wang, S.; Tsai, H.-L.; Streib, W. E.; Christou, G.; Hendrickson, D. N. *J. Chem. Soc., Chem. Commun.* **1992**, 1427.
(27) Wang, S.; Tsai, H.-L.; Libby, E.; Folting, K.; Streib, W. E.; Hendrickson, D. N.; Christou, G. *Inorg. Chem.* **1996**, *35*, 7578.

seventh carboxylate ligand located on two Jahn−Teller axes of the central two Mn^{III} ions and is thus more labile and susceptible to electrophilic attack than the other carboxylate groups. In an earlier paper,[28] we showed that this carboxylate ligand in $(NBu^n_4)[Mn_4O_2(O_2CPh)_7(pic)_2]$ can be selectively removed with 1 equiv of Me_3SiCl. Thus, complex **14** was treated in MeCN with 1 equiv of HNO_3, and dark orange microcrystals formed upon addition of Et_2O. Infrared and ^1H NMR spectroscopies (vide infra), as well as elemental analysis, were consistent with $[Mn_4O_2(NO_3)(O_2CEt)_6(bpy)_2]$-$(ClO_4)$ (**15**) as in eq 7. However, it was not clear whether

$$[Mn_4O_2(O_2CEt)_7(bpy)_2](ClO_4) + HNO_3 \rightarrow$$
$$[Mn_4O_2(NO_3)(O_2CEt)_6(bpy)_2](ClO_4) + EtCO_2H \quad (7)$$
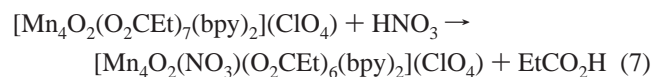
the NO_3^- ion was bound to the manganese, or merely a second, noncoordinated counterion. This point is of biological relevance since it is known that NO_3^- might bind to the Mn complex of PSII, partially restoring the catalytic activity of Cl^--depleted samples.[16] However, the crystal structure of complex **15** (vide infra) revealed a $\eta^1:\eta^1:\mu$-NO_3^- group bound to the two central manganese atoms in the same mode as that of the displaced $EtCO_2^-$ ligand. This reaction of **14** with HNO_3 thus represents a third method for the selective substitution of bridging carboxylate ligands by nitrate in manganese clusters.

Description of Structures. Selected interatomic distances and angles for complexes **7** and **15** are listed in Tables 2−4; ORTEP representations are presented in Figures 2 and 3.

The structure of **7** (Figure 2) consists of a $Mn^{III}_3Mn^{IV}$ trigonal pyramid with the Mn^{IV} ion at the apex. Each vertical Mn_3 face is capped by a μ_3-O^{2-} ion, and the basal Mn_3 face is capped by a $\eta^1:\mu_3$-NO_3^- ion. Three bridging $MeCO_2^-$ groups and three chelating Et_2dbm^- groups provide the peripheral ligation and make each Mn ion six-coordinate. As expected for high-spin Mn^{III} in near-octahedral geometry, the three Mn^{III} ions display Jahn−Teller distortions, and these take the form of elongations along the axes containing the NO_3^- group. The overall structure of **7** is similar to that of previous $[Mn_4O_3X(O_2CMe)_3(dbm)_3]$ complexes except for the X^- being NO_3^- for the first time. The $\eta^1:\mu_3$-NO_3^- is in an unusual bridging mode for this group; we have found no other example of a $\eta^1:\mu_3$-NO_3^- group, triply bridging modes for this ion usually involving η^2 or η^3 ligation. There are, however, $\eta^1:\mu_4$-NO_3^- groups known in the clusters $[V_4O_8$-$(NO_3)(tca)_4]^{2-}$ (tca = thiophene-2-carboxylate) and $[V_4O_8$-$(NO_3)(O_2CMe)_4]^-$.[29−31]

A comparison of the core dimensions of **7** with those for the $X^- = MeCO_2^-$ (**1**) and Cl^- (**3**) complexes reported elsewhere[23,27] is provided in Table 3. The μ_3-NO_3^- group causes little change in the core compared with **1** and **3**: the

(28) Libby, E.; Folting, K.; Huffman, C. J.; Huffman, J. C.; Christou, G. *Inorg. Chem.* **1993**, *32*, 2549.
(29) Heinrich, D. D.; Folting, K.; Streib, W. E.; Huffman, J. C.; Christou, G. *J. Chem. Soc., Chem. Commun.* **1989**, 1411.
(30) Arrowsmith, S.; Dove, M. F. A.; Logan, N.; Antipin, M. Y. *J. Chem. Soc., Chem. Commun.* **1995**, 627.
(31) Karet, G. B.; Sun, Z. M.; Heinrich, D. D.; McCusker, J. K.; Folting, K.; Streib, W. E.; Huffman, J. C.; Hendrickson, D. N.; Christou, G. *Inorg. Chem.* **1996**, *35*, 6450.

Table 2. Selected Interatomic Distances (Å) and Angles (deg) for **7**

Mn(1)	Mn(2)	2.798(3)	Mn(2)	O(25)	1.894(8)
Mn(1)	Mn(3)	2.790(2)	Mn(3)	O(5)	1.945(7)
Mn(1)	Mn(4)	2.775(2)	Mn(3)	O(6)	1.935(7)
Mn(2)	Mn(3)	3.226(2)	Mn(3)	O(8)	2.344(4)
Mn(2)	Mn(4)	3.261(2)	Mn(3)	O(19)	2.125(5)
Mn(3)	Mn(4)	3.201(2)	Mn(3)	O(42)	1.911(8)
Mn(1)	O(5)	1.851(9)	Mn(3)	O(46)	1.894(8)
Mn(1)	O(6)	1.847(7)	Mn(4)	O(6)	1.933(3)
Mn(1)	O(7)	1.874(5)	Mn(4)	O(7)	1.932(7)
Mn(1)	O(9)	1.910(7)	Mn(4)	O(8)	2.329(8)
Mn(1)	O(13)	1.947(9)	Mn(4)	O(15)	2.132(9)
Mn(1)	O(17)	1.927(4)	Mn(4)	O(63)	1.882(8)
Mn(2)	O(5)	1.916(6)	Mn(4)	O(67)	1.896(4)
Mn(2)	O(7)	1.946(9)	O(8)	N(84)	1.313(12)
Mn(2)	O(8)	2.301(7)	O(85)	N(84)	1.226(14)
Mn(2)	O(11)	2.159(7)	O(86)	N(84)	1.210(15)
Mn(2)	O(21)	1.898(5)			

O(5)	Mn(1)	O(6)	86.2(3)	O(8)	Mn(3)	O(19)	164.29(27)
O(5)	Mn(1)	O(7)	85.0(3)	O(8)	Mn(3)	O(42)	90.73(24)
O(5)	Mn(1)	O(9)	93.6(3)	O(8)	Mn(3)	O(46)	101.22(21)
O(5)	Mn(1)	O(13)	179.4(3)	O(19)	Mn(3)	O(42)	98.09(22)
O(5)	Mn(1)	O(17)	92.00(27)	O(19)	Mn(3)	O(46)	91.57(26)
O(6)	Mn(1)	O(7)	86.29(25)	O(42)	Mn(3)	O(46)	91.4(3)
O(6)	Mn(1)	O(9)	179.47(13)	O(6)	Mn(4)	O(7)	82.35(24)
O(6)	Mn(1)	O(13)	93.1(3)	O(6)	Mn(4)	O(8)	80.97(26)
O(6)	Mn(1)	O(17)	93.52(26)	O(6)	Mn(4)	O(15)	90.02(26)
O(7)	Mn(1)	O(9)	94.22(26)	O(6)	Mn(4)	O(63)	92.67(25)
O(7)	Mn(1)	O(13)	94.91(28)	O(6)	Mn(4)	O(67)	169.4(4)
O(7)	Mn(1)	O(17)	177.0(4)	O(7)	Mn(4)	O(8)	77.8(3)
O(9)	Mn(1)	O(13)	87.0(3)	O(7)	Mn(4)	O(15)	87.7(3)
O(9)	Mn(1)	O(17)	85.96(25)	O(7)	Mn(4)	O(63)	173.8(3)
O(13)	Mn(1)	O(17)	88.07(27)	O(7)	Mn(4)	O(67)	93.52(26)
O(5)	Mn(2)	O(7)	81.34(28)	O(8)	Mn(4)	O(15)	163.78(20)
O(5)	Mn(2)	O(8)	80.07(23)	O(8)	Mn(4)	O(63)	105.1(3)
O(5)	Mn(2)	O(11)	89.55(26)	O(8)	Mn(4)	O(67)	88.6(3)
O(5)	Mn(2)	O(21)	174.6(3)	O(8)	N(84)	O(85)	120.3(11)
O(5)	Mn(2)	O(25)	91.9(3)	O(8)	N(84)	O(86)	115.2(9)
O(7)	Mn(2)	O(8)	78.23(27)	O(15)	Mn(4)	O(63)	88.7(3)
O(7)	Mn(2)	O(11)	87.7(3)	O(15)	Mn(4)	O(67)	99.62(27)
O(7)	Mn(2)	O(21)	95.78(26)	O(63)	Mn(4)	O(67)	92.00(25)
O(7)	Mn(2)	O(25)	173.15(24)	O(85)	N(84)	O(86)	124.4(10)
O(8)	Mn(2)	O(11)	163.6(4)	Mn(1)	O(5)	Mn(2)	95.94(18)
O(8)	Mn(2)	O(21)	94.85(23)	Mn(1)	O(5)	Mn(3)	94.6(4)
O(8)	Mn(2)	O(25)	99.42(28)	Mn(2)	O(5)	Mn(3)	113.33(25)
O(11)	Mn(2)	O(21)	94.97(26)	Mn(1)	O(6)	Mn(3)	95.0(3)
O(11)	Mn(2)	O(25)	93.6(3)	Mn(1)	O(6)	Mn(4)	94.4(3)
O(21)	Mn(2)	O(25)	90.8(3)	Mn(3)	O(6)	Mn(4)	111.7(4)
O(5)	Mn(3)	O(6)	81.3(3)	Mn(1)	O(7)	Mn(2)	94.17(14)
O(5)	Mn(3)	O(8)	78.42(21)	Mn(1)	O(7)	Mn(4)	93.6(3)
O(5)	Mn(3)	O(19)	88.18(25)	Mn(2)	O(7)	Mn(4)	114.4(4)
O(5)	Mn(3)	O(42)	92.6(3)	Mn(2)	O(8)	Mn(3)	87.96(16)
O(5)	Mn(3)	O(46)	176.0(3)	Mn(2)	O(8)	Mn(4)	89.54(26)
O(6)	Mn(3)	O(8)	80.55(24)	Mn(2)	O(8)	N(84)	129.5(7)
O(6)	Mn(3)	O(19)	89.44(24)	Mn(3)	O(8)	Mn(4)	86.48(27)
O(6)	Mn(3)	O(42)	170.2(3)	Mn(3)	O(8)	N(84)	127.7(5)
O(6)	Mn(3)	O(46)	94.7(3)	Mn(4)	O(8)	N(84)	122.6(4)

Table 3. Comparison of Selected Interatomic Distances (Å) and Angles (deg) for $[Mn_4O_3X]^{6+}$ Complexes **1**, **3**, and **7**^{a}

parameter^b	X = $MeCO_2^-$ (**1**)	X = NO_3^- (**7**)	X = Cl^- (**3**)
Mn^{III}···Mn^{IV}	2.799	2.788	2.795
Mn^{III}···Mn^{II}	3.201	3.229	3.251
Mn^{III}−O$_b$	1.933	1.935	1.933
Mn^{IV}−O$_b$	1.867	1.857	1.864
Mn^{III}−X	2.299	2.325	2.650
Mn^{III}−X−Mn^{II}	88.2	87.99	75.7
Mn^{III}−O$_b$−Mn^{II}	111.8	113.14	114.5
Mn^{III}−O$_b$−Mn^{IV}	94.8	94.62	94.8

^{a} Averaged under idealized C_{3v} symmetry. ^{b} b = bridging mode.

only significant differences are to be found in Mn−X distances and Mn^{III}−X−Mn^{III} angles, with a slight influence
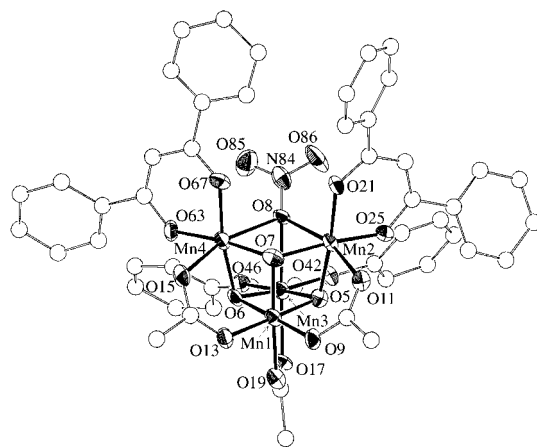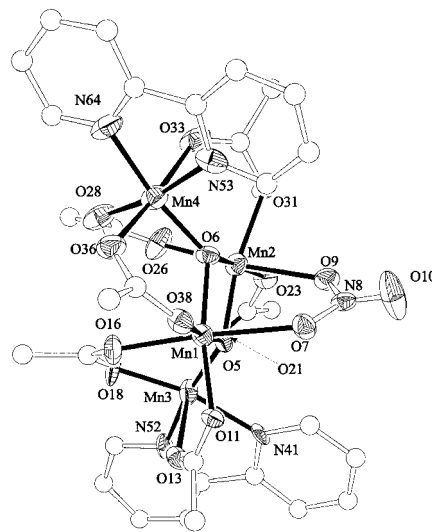
Table 4. Interatomic Distances (Å) and Angles (deg) for **15**

Mn(1)	Mn(2)	2.854(3)	Mn(3)	O(13)	2.201(9)
Mn(1)	O(5)	1.900(8)	Mn(3)	O(18)	1.916(8)
Mn(1)	O(6)	1.894(8)	Mn(3)	O(21)	2.143(9)
Mn(1)	O(7)	2.351(9)	Mn(3)	N(41)	2.056(11)
Mn(1)	O(11)	1.955(9)	Mn(3)	N(52)	2.033(11)
Mn(1)	O(16)	2.133(9)	Mn(4)	O(6)	1.858(8)
Mn(1)	O(38)	1.942(9)	Mn(4)	O(28)	1.926(11)
Mn(2)	O(5)	1.896(8)	Mn(4)	O(33)	2.137(10)
Mn(2)	O(6)	1.864(8)	Mn(4)	O(36)	2.117(10)
Mn(2)	O(9)	2.317(9)	Mn(4)	N(53)	2.057(12)
Mn(2)	O(23)	1.942(8)	Mn(4)	N(64)	2.010(12)
Mn(2)	O(26)	2.123(10)	O(7)	N(8)	1.276(12)
Mn(2)	O(31)	1.959(9)	O(9)	N(8)	1.286(12)
Mn(3)	O(5)	1.844(8)	O(10)	N(8)	1.183(13)

O(5)	Mn(1)	O(6)	81.0(4)	O(13)	Mn(3)	N(41)	82.0(4)
O(5)	Mn(1)	O(7)	88.2(3)	O(13)	Mn(3)	N(52)	88.4(4)
O(5)	Mn(1)	O(11)	97.4(4)	O(18)	Mn(3)	O(21)	99.0(4)
O(5)	Mn(1)	O(16)	91.0(4)	O(18)	Mn(3)	N(41)	167.3(4)
O(5)	Mn(1)	O(38)	175.7(4)	O(18)	Mn(3)	N(52)	91.1(4)
O(6)	Mn(1)	O(7)	84.8(3)	O(21)	Mn(3)	N(41)	87.3(4)
O(6)	Mn(1)	O(11)	169.4(4)	O(21)	Mn(3)	N(52)	85.5(4)
O(6)	Mn(1)	O(16)	99.3(4)	N(41)	Mn(3)	N(52)	78.3(4)
O(6)	Mn(1)	O(38)	94.7(4)	O(6)	Mn(4)	O(28)	96.7(4)
O(7)	Mn(1)	O(11)	84.6(3)	O(6)	Mn(4)	O(33)	91.7(3)
O(7)	Mn(1)	O(16)	175.6(4)	O(6)	Mn(4)	O(36)	94.7(4)
O(7)	Mn(1)	O(38)	90.7(3)	O(6)	Mn(4)	N(53)	91.7(5)
O(11)	Mn(1)	O(16)	91.2(4)	O(6)	Mn(4)	N(64)	169.7(5)
O(11)	Mn(1)	O(38)	86.7(4)	O(28)	Mn(4)	O(33)	89.6(4)
O(16)	Mn(1)	O(38)	90.3(4)	O(28)	Mn(4)	O(36)	96.0(4)
O(5)	Mn(2)	O(6)	81.9(3)	O(28)	Mn(4)	N(53)	170.1(5)
O(5)	Mn(2)	O(9)	85.4(3)	O(28)	Mn(4)	N(64)	93.3(5)
O(5)	Mn(2)	O(23)	95.0(4)	O(33)	Mn(4)	O(36)	171.0(4)
O(5)	Mn(2)	O(26)	100.0(4)	O(33)	Mn(4)	N(53)	85.0(4)
O(5)	Mn(2)	O(31)	167.8(4)	O(33)	Mn(4)	N(64)	85.9(4)
O(6)	Mn(2)	O(9)	89.0(3)	O(36)	Mn(4)	N(53)	88.4(4)
O(6)	Mn(2)	O(23)	176.5(4)	O(36)	Mn(4)	N(64)	86.6(4)
O(6)	Mn(2)	O(26)	91.4(4)	N(53)	Mn(4)	N(64)	78.1(6)
O(6)	Mn(2)	O(31)	96.0(4)	O(7)	N(8)	O(9)	117.3(11)
O(9)	Mn(2)	O(23)	89.0(3)	O(7)	N(8)	O(10)	120.3(12)
O(9)	Mn(2)	O(26)	174.6(4)	O(9)	N(8)	O(10)	122.0(12)
O(9)	Mn(2)	O(31)	82.5(3)	Mn(1)	O(5)	Mn(2)	97.5(4)
O(23)	Mn(2)	O(26)	90.9(4)	Mn(1)	O(5)	Mn(3)	120.7(4)
O(23)	Mn(2)	O(31)	86.6(4)	Mn(2)	O(5)	Mn(3)	128.1(4)
O(26)	Mn(2)	O(31)	92.1(4)	Mn(1)	O(6)	Mn(2)	98.9(4)
O(5)	Mn(3)	O(13)	94.4(3)	Mn(1)	O(6)	Mn(4)	125.2(4)
O(5)	Mn(3)	O(18)	98.2(4)	Mn(2)	O(6)	Mn(4)	123.9(4)
O(5)	Mn(3)	O(21)	90.1(4)	Mn(1)	O(7)	N(8)	129.2(8)
O(5)	Mn(3)	N(41)	92.9(4)	Mn(2)	O(9)	N(8)	129.2(8)
O(5)	Mn(3)	N(52)	170.3(4)	O(7)	N(8)	O(9)	117.3(11)
O(13)	Mn(3)	O(18)	90.7(4)	O(7)	N(8)	O(10)	120.3(12)
O(13)	Mn(3)	O(21)	168.6(3)	O(9)	N(8)	O(10)	122.0(12)

Figure 2. ORTEP representation of **7** at the 50% probability level. For clarity, the ethyl groups of the Et$_2$dbm ligands are not shown.

Figure 3. ORTEP representation of **15** at the 40% probability level.

EtCO$_2^-$ groups, a NO$_3^-$ ligand, and two bpy chelates. Each of the carboxylate groups is bridging a body−wingtip Mn$_2$ pair, while the nitrate anion is bridging the "body" manganese ions in a η^1:η^1:μ-NO$_3^-$ fashion. This binding mode for nitrate is often encountered in complexes of copper[33] but finds no precedent in molecular manganese chemistry; however, there exists a polymeric Mn^{III} chain with bridging η^1:η^1:μ-NO$_3^-$ groups.[34] The bpy ligands chelate the two wingtip Mn ions Mn3 and Mn4. The cluster possesses virtual C_2 symmetry. Charge considerations indicate the oxidation state +3 for all four metals; the presence of Jahn−Teller distortion taking the form of two longer trans bonds (av 2.192 Å) at each Mn center supports this hypothesis. Owing to the heterogeneous nature of the donor environment around Mn3 and Mn4, the equatorial bond distances at these centers (av Mn−N = 2.039 Å, av Mn−O = 1.886 Å) are more disperse than those at the body Mn ions (av 1.920 Å). The [Mn$_4$(μ_2-O)$_2$]$^{8+}$ core contains four different types

also on Mn^{III}−O$_b$−Mn^{III} angles. Thus, the μ_3-NO$_3^-$ and μ_3-MeCO$_2^-$ groups give essentially congruent cores, while the larger size of Cl$^-$ leads to greater differences.

The structure of **8**·hexane (not shown but available; see the Supporting Information) is very similar to that of the related butterfly complex [Mn$_4$O$_2$(O$_2$CMe)$_6$(py)$_2$(dbm)$_2$][23] and contains a [Mn$^{III}_4$(μ_3-O)$_2$]$^{8+}$ core with bridging carboxylate and chelating dbm groups on the periphery. It differs in that **8** has no py groups, the latter completing octahedral geometry at the central Mn ions of [Mn$_4$O$_2$(O$_2$CMe)$_6$(py)$_2$-(dbm)$_2$]. Thus, the two body Mn^{III} ions in **8** are five-coordinate with a geometry lying between a trigonal bipyramid (tbp) and a square pyramid (sp).[32]

The cation of **15** (Figure 3) contains four Mn atoms in a butterfly-like arrangement, bridged by two μ_3-oxide ions. Approximately octahedral coordination at each Mn is completed by the peripheral ligands, which consist of six

(32) Addison, A. W.; Rao, T. N.; Reedijk, J.; Rijn, J. V.; Verschoor, G. C. *J. Chem. Soc., Dalton Trans.* **1984**, 1349.
(33) Hendriks, H. M. J.; Birker, J. M. W. L.; Rijn, J. V.; Verschoor, G. C.; Reedijk, J. *J. Am. Chem. Soc.* **1982**, *104*, 3607.
(34) Shyu, H.-L.; Wei, H.-H.; Wang, Y. *Inorg. Chim. Acta* **1999**, *290*, 8.

Table 5. ^{1}H NMR Spectral Data[a] for Complexes **1−7** and **9−12** in CDCl$_3$

complex	Me (μ_3)	Me	CH$_2$*CH$_3$*	*CH$_2$*CH$_3$	R$_2$dbm⁻					
					o-H	*m*-H	*p*-H	CH	CH$_2$	CH$_3$
1	~58	37.9			~1.5	5.3	−0.87	73		
2	~56	37.8			~1.9	5.0		78	11.35	1.20
3		41.6			n.o.	5.0	−1.50	76		
4		41.5			n.o.	5.1	−1.58	77		
5		37.6			~1.5	5.3	−0.61	72		
6		37.4			~1.6	5.2	−0.83	77		
7		36.9			~1.8	4.9		82	11.36	1.21
9			8.8	28.2	~0.8	5.1	−1.17	74		
10			8.7	28.9	n.o.	5.2	−1.25	75		
11			7.6	24.8	n.o.	5.3	−0.31	68		
12			7.4	27.3	~1.9	5.3	−0.55	74		

[a] The data are the chemical shifts (ppm) on the δ scale. Shifts downfield are positive. Very broad peaks are given to one decimal place or to the nearest integer. n.o. = not observed (too broad or obscured by solvent peaks).

of Mn···Mn vectors: Mn1 and Mn2 are 2.854 Å apart, the body Mn centers are separated from the wingtip ions by averages of 3.292 Å (two carboxylate bridges) and 3.325 Å (one carboxylate), and the Mn3···Mn4 distance is 5.495 Å. The overall structures of compounds **8** and **15** are similar to those of other previously reported clusters with the [Mn$_4$O$_2$]$^{8+}$ core,[18,21−23] providing new entries to the available database of related Mn$_4$ complexes for identifying possible correlations between structure and other properties. In a recent paper we have reported a comparison between the core parameters of complex **15** and other previously characterized clusters with the same topology.[18] Complex **15** is the first example of this family of compounds possessing a bridging ligand other than carboxylate.

^{1}H NMR Spectroscopy. All complexes presented in this work have been investigated by ^{1}H NMR spectroscopy. These studies have been conducted to determine whether the solid-state structure of these molecules is retained in solution. In addition, NMR has represented a useful tool to monitor the various transformations discussed in the synthetic section, and the purity of the products. The spectra of all complexes except **8** have been interpreted, and lists of the observed chemical shifts are presented in Tables 5 (complexes **1−7** and **9−12**) and 6 (complexes **13−15**). Some of the collected spectra are depicted in Figures 4−6.

The interpretation of the spectra of complexes **13** and **14** (Figure 4, top) has benefited from previous NMR studies performed on the acetate analogues,[21,22] which involved the use of deuterated acetate ligands, spin−lattice relaxation time measurements, and alkyl substitutions on the rings of the bpy ligand. Both compounds display very similar patterns, with the main differences caused by the nature of the chelating ligand. The observed chemical shifts span a large range (up to ~190 ppm wide), consistent with the presence of a large magnetic moment within the molecules[21,22] (vide infra). Upon inspection, the spectra indicate effective C_2 symmetry for each complex, consistent with the solid-state structures previously observed for the acetate analogues of these two complexes.[21,22] Thus, complexes **13** and **14** each display four sets of signals in a 2:2:2:1 integration ratio for the four inequivalent types of μ_2-O$_2$CCH$_2$CH$_3$⁻ groups. The spectrum of **15** (Figure 4, bottom) shows that **15** is the result of removing the unique carboxylate ligand from **14** (reso-

Table 6. ^{1}H NMR Spectral Data for Complexes **13−15**

resonance[a]	**13**[b,c]	**14**	**15**
Me	3.63	3.81	4.35
Me	2.19	2.45	2.99
Me	1.94	1.38	0.66
Me	1.36	4.49	
C⁺	1.10		
CH$_2$	51.96	52.17	52.64
	45.20	47.52	51.89
CH$_2$	43.62	44.27	44.45
	42.39	42.96	43.29
CH$_2$	37.04	38.51	42.11
	27.09	31.48	32.73
CH$_2$	22.15	24.68	
	19.75	22.64	
L−L	32.02	34.81	31.74
L−L	−5.74	20.43	19.64
L−L	−16.49	−9.17	−12.43
L−L	−50.30	−17.99	−19.75
L−L		−18.99	−21.36
L−L		−29.85	−31.09
L−L		−69.84	−82.22
L−L		−127.94	−136.53

[a] Me and Me′ are methyl groups from body−wingtip and body−body MeCH$_2$CO$_2$⁻ groups, respectively. CH$_2$ and CH$_2$′ are methylene groups (diastereotopic) from body−wingtip and body−body MeCH$_2$CO$_2$⁻ groups, respectively. L−L is the chelating ligand. [b] The data are the chemical shifts (ppm) on the δ scale. Shifts downfield are positive. [c] Peaks from the cation and those from propionate Me groups are not resolved.

nances a′ and b′ in Figure 4, top). Thus, complex **15** shows a spectrum with the same characteristics as those for **13** and **14** but with only three sets of propionate signals with equal integration ratios. The methylene signals from the propionate groups appear as two peaks, revealing their diastereotopic nature, and show no resolved spin−spin coupling. This, together with their large isotropic shift (10−60 ppm), underscores the influence of the paramagnetic metals on the magnetic environment of these nuclei. On the other hand, the signals of the corresponding methyl groups appear as broad singlets with a dramatically smaller chemical shift (0−5 ppm). These have been clearly identified for complexes **14** and **15**. In complex **13**, these signals are found together with the peaks of the counterion (NBu$^n_4$)⁺ of the cluster, and individual assignments could not be made.

The C_2 symmetry of these molecules is also reflected in the resonances for the chelating ligands. In all cases, only one set of signals is present for the chelates while all protons within each ligand appear as inequivalent. Thus, eight signals are observed for the bpy ligands, while the presence of
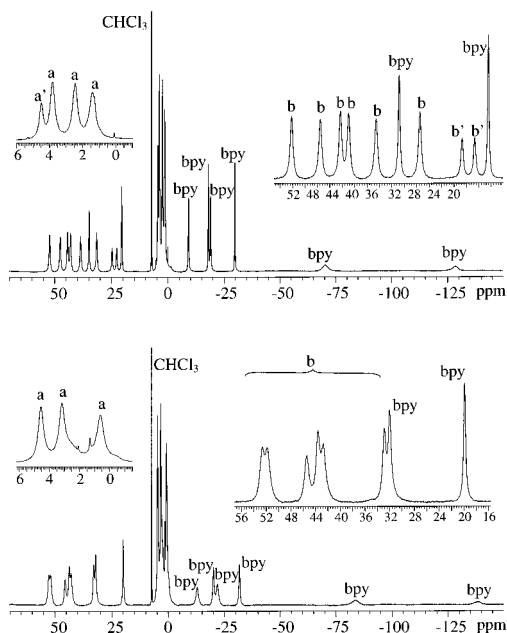
Figure 4. ¹H NMR (300 MHz) spectra of **14** (top) and **15** (bottom) in CDCl₃. The resonances marked a and b are for methyl and methylene, respectively, from the propionate ligands.
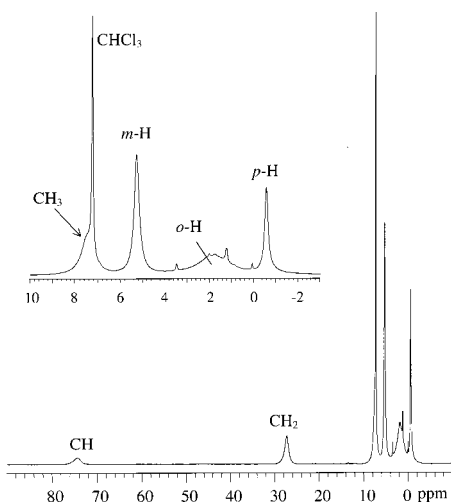

Figure 5. ¹H NMR (300 MHz) spectrum of **12** in CDCl₃.

picolinate gives rise to four resonances. The line broadenings of the different signals are very disparate, as expected from the range of distances to the manganese centers. In addition, the fact that signals from the chelate rings display strong paramagnetic shifts to either side of the diamagnetic region indicates that a π-spin-delocalization mechanism is operative in the coupling of the nuclear magnetic moment with the unpaired electrons.[35]

The ¹H NMR spectra of the family of complexes [Mn₄O₃X(O₂CR′)₃(R₂dbm)₃] (X = O₂CMe, Cl, Br, F, NO₃; R′ = Me and R = H, **1** and **3−6**; R′ = Et and R = H, **9−12**; R′ = Me and R = Et, **2** and **7**) show that the virtual C_{3v} symmetry that they display in the solid state is retained in solution (Figures 5 and 6, Table 5). Thus, all these clusters

(35) *NMR of Paramagnetic Molecules*; La Mar, G. N., Horrocks, W. D., Jr., Holm, R. H., Eds.; Academic Press: New York, 1973.
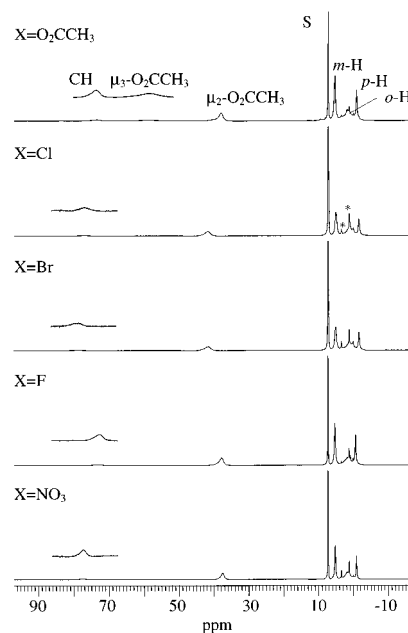
Figure 6. ¹H NMR (300 MHz) spectra of complexes **1** and **3−6** in CDCl₃.

possess three magnetically equivalent μ_2-O₂CR⁻ groups that manifest themselves in the ¹H NMR spectrum as a single resonance (R′ = Me) or as a pair of resonances (R′ = Et). Also, only one group of signals for the three equivalent dbm ligands is observed. The μ_2-O₂CMe⁻ groups appear as a relaxation-broadened, paramagnetically shifted signal (37−42 ppm) (Figure 6). The assignment of this resonance is supported by comparison with the ²H NMR spectra of the deuterioacetate analogues of some of these complexes[14] (vide supra). The two protons of the EtCO₂⁻ methylene groups are not diastereotopic, and therefore give a single signal with a large isotropic shift (24−28 ppm). The protons of the corresponding methyl groups are one bond further from the metal centers and therefore are subject to a much smaller paramagnetic shift (7−9 ppm).

All the resonances from the three equivalent R₂dbm⁻ ligands have been assigned. The methine hydrogen is the closest to the manganese centers and results in the broadest resonance (broadness αr^{-6}, where r is the Mn···H distance), which is located at $\delta = 60−80$ ppm. The second closest hydrogens to Mn are the o-H atoms of the phenyl rings. This peak appears upfield ($\delta = 1−2$ ppm) of its diamagnetic position and is significantly broadened, often obscured by solvent signals. The resonance for the p-H atoms is observed in the $\delta = −0.3$ to $−1.6$ ppm region, and disappears upon alkyl substitution. The m-H signals have twice the integration of the p-H signals, and are found between $\delta = 4.8$ ppm and $\delta = 5.3$ ppm. The p-Et groups of the phenyl rings represent a good NMR probe when the reactivity of the cubane complexes is monitored or the purity of the products is assessed because the chemical shift of the CH₂ group is sensitive to the type of complex ($\delta = \sim11.3$ ppm for [Mn₄O₃X] complexes) and is easily detected. On the other hand, the chemical shift of the methyl hydrogens of this substituent remains almost unchanged from its diamagnetic value (~1.2 ppm).
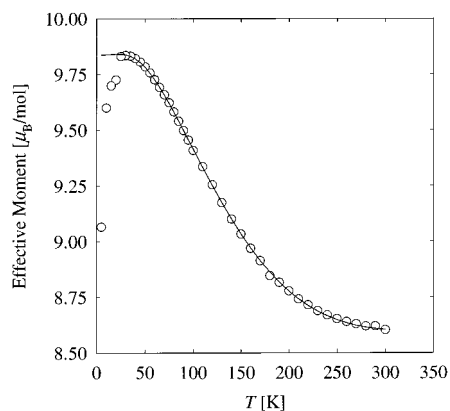
Figure 7. Effective magnetic moment (μ_{eff}) per molecule vs T for **12** in a 10.0 kG field. The solid line is a fit of the 30−300 K data to the appropriate theoretical equation; see the text for the fitting parameters.
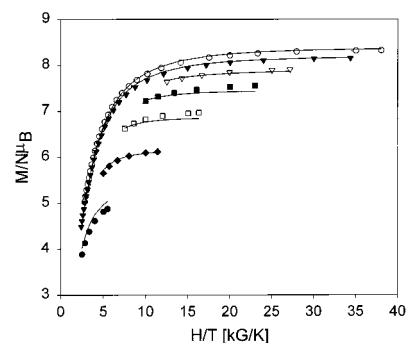

Figure 8. $M/N\mu_{\text{B}}$ vs H/T for **12** at 10 (●), 20 (◆), 30 (□), 40 (■), 50 (▽), 60 (▼), and 70 (○) kG. The solid lines are the fits to the theoretical magnetization; see the text for the fitting parameters.

Magnetic Susceptibility Study of 12. Variable-temperature bulk magnetization data were collected for complex **12**. These measurements were performed to determine the influence of nitrate within the series of $[Mn_4O_3X]^{6+}$ complexes, whose magnetic properties have been studied extensively.[11,12,14,23,24,26,27,36,37] The data were obtained from pressed microcrystalline samples in the 5−300 K range under a constant magnetic field of 10.0 kG. A plot of the effective magnetic moment, μ_{eff}, of complex **12** vs temperature is shown in Figure 7. The value of $\mu_{\text{eff}}/\mu_{\text{B}}$ ($\chi_{\text{m}}T/\text{cm}^3\cdot\text{K}\cdot\text{mol}^{-1}$) increases with decreasing temperature from 8.60 (9.25) at 300 K until a maximum of 9.84 (12.09) is reached at 30 K, followed by a sharper decrease at lower temperatures. This behavior indicates the presence of at least some ferromagnetic interactions between the spin centers of the complex, and the maximum of μ_{eff} (9.84) is close to the theoretical spin-only ($g = 2$) value for an isolated $S_{\text{T}} = \frac{9}{2}$ spin ground state (9.95). The exchange parameters within the cluster were obtained by fitting the experimental data to the appropriate theoretical expression of χ_{m} vs T. This expression has been derived previously,[38] using the Van Vleck equation,[39] for other $[Mn_4O_3X]^{6+}$ complexes that consist of a Mn_4 trigonal pyramid with C_{3v} symmetry. For this, the Heisenberg spin Hamiltonian given in eq 8 was used and modified by applying the Kambe vector coupling method[40] as described earlier.[41] This leads to the eigenvalue expression of eq 9,

$$\hat{H} = -2J_{33}(\hat{S}_2\hat{S}_3 + \hat{S}_2\hat{S}_4 + \hat{S}_3\hat{S}_4) - 2J_{34}(\hat{S}_1\hat{S}_2 + \hat{S}_1\hat{S}_3 + \hat{S}_1\hat{S}_4) \tag{8}$$

$$E(S_{\text{T}}) = -J_{33}[S_{\text{A}}(S_{\text{A}} + 1)] - J_{34}[S_{\text{T}}(S_{\text{T}} + 1) - S_{\text{A}}(S_{\text{A}} + 1)] \tag{9}$$

which gives the energy, $E(S_{\text{T}})$, of each of the possible total spin states, S_{T}, of the complex, where $S_{\text{A}} = S_2 + S_3 + S_4$

and $S_{\text{T}} = S_1 + S_{\text{A}}$. In eqs 8 and 9, J_{34} and J_{33} are the exchange parameters for the Mn^{III}/Mn^{IV} and Mn^{III}/Mn^{III} interactions, respectively, $S_2 = S_3 = S_4 = 2$ for the Mn^{III} centers, and $S_1 = \frac{3}{2}$ for the Mn^{IV} ion. The best fit (Figure 7, solid line) of the experimental points to the theoretical model was obtained with $J_{34} = -23.9$ cm^{-1}, $J_{33} = 4.9$ cm^{-1}, and $g = 1.98$, with the temperature-independent paramagnetism (TIP) parameter held constant at 600×10^{-6} cm$^3\cdot$mol^{-1}. This leads to an $S_{\text{T}} = \frac{9}{2}$ ground state for this complex, with $S_{\text{T}} = \frac{7}{2}$ as the first excited state lying 130.5 cm^{-1} above in energy. For this fit, only the experimental points above 30 K were used because low-temperature effects such as zero-field splitting (ZFS) and intermolecular exchange interactions, which are the likely cause of the decrease of μ_{eff} below 30 K, are not accommodated by the theoretical model. The parameters obtained for complex **12** are very similar to those obtained previously for similar $[Mn_4O_3X]^{6+}$ complexes, for which J_{33} and J_{34} values in the ranges 5.3−10.8 and −21 to −34 cm^{-1}, respectively, have been found.[11,12,14,23,26]

To confirm the $S_{\text{T}} = \frac{9}{2}$ ground state and to obtain the magnitude of the axial zero-field splitting parameter D, magnetization data were collected in the 1.70−30.0 K and 10−70 kG (1.0−7.0 T) ranges. The data are plotted as reduced magnetization ($M/N\mu_{\text{B}}$) vs H/T in Figure 8. They were fit to the theoretically calculated magnetization using the method described elsewhere, which incorporates a full powder average and assumes that only the ground state is populated.[42] The fits are shown as solid lines in Figure 8, and the fitting parameters were $S = \frac{9}{2}$, $D = -0.45(1)$ cm^{-1}, and $g = 1.96(1)$. The value of D is typical of the $[Mn_4O_3X]^{6+}$ family of complexes, being very similar, for example, to the $D = -0.47$ cm^{-1} determined for the $X^- = MeCO_2^-$ analogue.[23] The relatively large value of D also confirms the appropriateness of ignoring the low-temperature data of Figure 7 in the fit of μ_{eff} vs T since the model does not incorporate ZFS.

(36) Aubin, S. M. J.; Dilley, N. R.; Wemple, M. W.; Maple, M. B.; Christou, G.; Hendrickson, D. N. *J. Am. Chem. Soc.* **1998**, *120*, 839.
(37) Aubin, S. M. J.; Dilley, N. R.; Pardi, L.; Krzystek, J.; Wemple, M. W.; Brunel, L. C.; Maple, M. B.; Christou, G.; Hendrickson, D. N. *J. Am. Chem. Soc.* **1998**, *120*, 4991.
(38) Wang, S.; Tsai, H.-L.; Libby, E.; Folting, K.; Streib, W. E.; Hendrickson, D. N.; Christou, G. *Inorg. Chem.* **1996**, *35*, 7578.
(39) *The Theory of Electric and Magnetic Susceptibilities*; Van Vleck, J. H., Ed.; Oxford Univesity Press: London, 1932.

(40) Kambe, K. *J. Phys. Soc. Jpn.* **1950**, *5*, 48.
(41) Hendrickson, D. N.; Christou, G.; Schmitt, E. A.; Libby, E.; Bashkin, J. S.; Wang, S.; Tsai, H.-L.; Vincent, J. B.; Boyd, P. D. W.; Huffman, J. C.; Folting, K.; Li, Q.; Streib, W. E. *J. Am. Chem. Soc.* **1992**, *114*, 2455.
(42) Yoo, J.; Yamaguchi, A.; Nakano, M.; Krzystek, J.; Streib, W. E.; Brunel, L.-C.; Ishimoto, H.: Christou, G.; Hendrickson, D. N. *Inorg. Chem.* **2001**, *40*, 4604.

Discussion

In this work, a convenient method has been developed to obtain carboxylate-bridged tetranuclear manganese oxide aggregates in high yield from simple reagents. This method consists of generating Mn^{III}/Mn^{IV} ions in situ in aqueous carboxylic acid (acetic or propionic acid) in the presence of a chelating ligand. The Mn^{III}/Mn^{IV} ions are produced via comproportionation between MnO_4^- and Mn^{II} sources, as summarized in eqs 10 (complex **1**) and 11

$$Mn^{VII} + 3Mn^{II} \rightarrow Mn^{III}{}_3Mn^{IV} \qquad (10)$$

$$Mn^{VII} + 4Mn^{II} \rightarrow 5Mn^{III} \qquad (11)$$
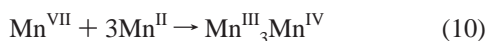
(complexes **8**, **13**, and **14**). From this system, the tetranuclear complex precipitates either spontaneously (dbm complexes; **1** and **8**) or upon addition of Et_2O (bpy or pic complexes; **13** and **14**, respectively) in high yield and purity. The use of a carboxylic acid as a solvent stabilizes the carboxylate-bridged cluster against hydrolysis, despite the large amounts of water ($\sim$10%) present in the reaction system. For the dbm systems, two very different compounds are isolated depending on the nature of the carboxylate. When acetate is used, a highly distorted cubane complex with a $[Mn_4O_3(O_2CMe)]^{6+}$ core (**1**) is obtained. In contrast, a butterfly-type complex with a $[Mn^{III}{}_4O_2]^{8+}$ core (**8**) precipitates when the carboxylate is propionate. This experimental difference is rationalized in terms of solubility properties. It is possible that the formation of **1** occurs through the intermediacy of a $[Mn^{III}{}_4O_2]^{8+}$ complex similar to **8** (as suggested by the original preparation of **1**, vide supra),[23] which would not precipitate. In the propionate system, complex **8** precipitates before further oxidation to the $Mn^{III}{}_3Mn^{IV}$ product can take place.

Acidolysis of the carboxylate-bridged cluster $[Mn_4O_3$-$(O_2CMe)_4(dbm)_3]$ (**1**) with concentrated aqueous mineral acids HX (X = F, Cl, Br, NO_3) has proven to be a convenient method to access the corresponding μ_3-X-bridged cubane clusters $[Mn_4O_3X(O_2CMe)_3(dbm)_3]$. These reactions occur via the selective protonation of the unique μ_3-O_2CMe ligand of complex **1** and substitution of this group by the corresponding μ_3-X ligand. The solvent in which these reactions take place (CH_2Cl_2) does not favor the formation of charged species. (Reactions in more polar MeCN and similar solvents are precluded by the very low solubility of **1**; reaction of a slurry of **1** in MeCN with mineral acids at the stoichiometry used in CH_2Cl_2 gave essentially no reaction.) We believe that the substitutions proceed by protonation of the μ_3-O_2CMe group at its exposed O atom, making it a good leaving group, during a dissociative interchange step, perhaps through an intermediate as shown in Scheme 1, to give a μ_3-X^- and acetic acid.

Acidolysis has also proven to be a good way to remove μ_2-O_2CEt groups from $[Mn_4O_2]^{8+}$ complexes and promote cluster rearrangement. The transformation of $[Mn_4O_2$-$(O_2CEt)_6(dbm)_2]$ (**8**) into $[Mn_4O_3X(O_2CEt)_3(dbm)_3]$ (X = Cl, **9**; Br, **10**; F, **11**; NO_3, **12**) upon reaction with the corresponding acid HX is analogous to previously described reactions of the complex $[Mn_4O_2(O_2CMe)_6(py)_2(dbm)_2]$ with

Scheme 1
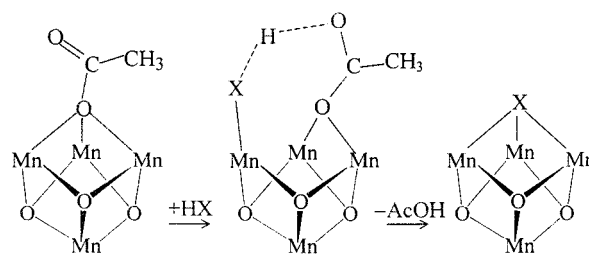
trimethylsilyl reagents.[11,26,27] In these transformations, the rearrangement was triggered by the reaction of Me_3SiX (Cl, Br, N_3, NCO) with one carboxylate from the $[Mn_4O_2]^{8+}$ complex, the μ_3-X-bridged complexes $[Mn_4O_3X(OAc)_3$-$(dbm)_3]$ being the isolated products. These two types of reactions demonstrate that all six of the carboxylate ligands are important for the stability of the butterfly-type complexes $[Mn_4O_2(O_2CMe)_6(py)_2(dbm)_2]$ and $[Mn_4O_2(O_2CEt)_6(dbm)_2]$. However, in the formation of $[Mn_4O_2(NO_3)(O_2CEt)_6(bpy)_2]$-$(ClO_4)$ (**15**), the substitution of the seventh bridging carboxylate group by a μ-NO_3 ligand on a $[Mn_4O_2]^{8+}$ complex has been achieved for the first time (eq 7). As shown here and in a previous example,[28] removal or substitution of a carboxylate ligand from a butterfly-type complex with preservation of the overall structure is only possible if a seventh carboxylate group, bridging the central Mn atoms, is present. This unique carboxylate group is the most labile of all since it is the only one bound to Mn on two Jahn–Teller positions. Its presence is not essential to maintain the structure of the complex.

The reactions in this work of carboxylate-bridged manganese clusters with nitrate have biological relevance, since the presence of NO_3^- has interesting effects on the structure and activity of PSII.[16] An important question to elucidate is whether nitrate becomes a ligand of Mn in the WOC and under which conditions such binding would take place. We have shown that replacement of carboxylate ligands by nitrate can easily take place in tetranuclear manganese aggregates without changes in the structure when the leaving groups are located on the Jahn–Teller positions of Mn^{III} (eqs 3, 5, and 7). In other cases, it has been observed that simple substitution is not possible without severely altering the structure and properties of the complex (eq 6).

NMR spectroscopy has been extremely useful for the development of the synthetic work that has led to this paper. Interpretation of the spectra of all complexes presented here (except for the spectrum of **8**, which remains ambiguous) has confirmed that their solid-state structure and virtual symmetry are retained in $CDCl_3$ solution. The ^2H and ^1H NMR study presented in this work has benefited from extensive work previously reported for similar systems[14,21,22,27] and represents a significant contribution to a growing database on the spectroscopic properties of Mn aggregates as a function of structural type.

Using the new synthetic methods presented in this paper, access has been gained to a new member of the family of complexes with formula $[Mn_4O_3X(O_2CMe)_3(dbm)_3]$ containing a NO_3^- group in the μ_3-X position for the first time. In

previous papers, we have proposed these complexes as structural models for the S_2 state of the WOC in PSII. One of the major drawbacks for this proposition is that the spin state of all members of the family is $S = \frac{9}{2}$, too high to mimic the magnetic state of the complex in the native site (depending on the study, $S = \frac{1}{2}$, $\frac{3}{2}$, or $\frac{5}{2}$). As it has been further emphasized in this work with the magnetic susceptibility study of complex **12**, the nature of the μ_3-X group does not affect the value of the spin ground state of the cluster.

In summary, a number of original synthetic strategies have been developed, providing convenient access to a number of tetranuclear manganese clusters with interesting magnetic properties and biological relevance. Some of these complexes have been prepared for the first time during this work.

Supporting Information Available: X-ray crystallographic data in CIF format for the structures of complexes **7**, **8**, and **15**. This material is available free of charge via the Internet at http://pubs.acs.org.

IC0105617